A Geoinformatics Study of Forest Cover Changes in Erbil, Kurdistan Region of Iraq

Ragheb Kamal Mohammad [1*], Zahra Khaleq Abdulla [2]

[1] Department of Forestry, College of Agricultural Engineering Sciences, Salahaddin University-Erbil 44002, Kurdistan Region, Iraq
[2] Researcher, Erbil 44002, Kurdistan Region, Iraq

[*] Correspondence: ragheb.mohammad@su.edu.krd

Abstract

Several possible causes, such as rises in buildings, climate change, agricultural expansion, and forest fires, are expected to cause a decline in the trend of forest cover in the world. A categorical forest cover analysis was used alongside a random forest algorithm, a modern form of supervised machine learning in remote sensing, to assess forest cover change in four districts in the northeast of Erbil province between two thematic maps, 2003 and 2023. Training sample points were applied with a false color image downloaded from Landsat 7 and 9 images with 30 m resolution. All the spatial analysis and geoprocessing were performed using ArcGIS Pro tools. The output results of classification are evaluated using assessment accuracy and a confusion matrix. Our findings indicated that the forest cover shifted. The western part of the study area, which borders mostly with agricultural fields, experienced a decrease in tree cover, reaching 7.03%. The mergasur region and other districts experienced constant increases in tree cover due to sufficient precipitation and altitudes, resulting in a 6.79% net increase in forest cover over a period of two decades. The overall assessment accuracy was 88% in 2003, but increased to 93% in 2023. Researchers should conduct future studies using further advanced technology of remote sensing along with high-resolution images for ongoing monitoring and enhanced forest conservation in the region.

Keywords: forest cover change, remote sensing, Random Forest (RF), Erbil, deforestation

Introduction

Forests play an active role in climate control, protect biodiversity, preserving ecological stability and providing essential ecosystem services. It provides clean water and air, control soil fertility and erosion. It has noteworthy social and economic worth, supporting livelihoods, and supplying forest timbers. In addition, forests in the world are facing serious hazards such as forest loss, climate change, agricultural expansion, forest fires and urbanization [11, 24]. The Kurdistan region has a variety of forest ecosystems namely, natural oak forest, pistachio forest, and mixed oak and pine forests. They provide great habitats for a variety of plant as well as animal species [4,21]. Kurdistan located in a highland territory in north-eastern part of Iraq, expressed by a diverse landscape of forests, grasslands, and agricultural lands. The territory has accomplished serious forest cover damage in late decades due to numerous reasons, for instance overgrazing, forest fires, and agricultural expansion. Logging for agricultural sector, building and firewood uses are a main driver of forest loss in the region [17,33,35]. Furthermore, changing in climate condition has accelerated forest land degradation through expanded drought strain and wildfires in the nature. Also, it is expected due to climate change and effects the forest management systems [3,16]. The fluctuations in precipitation have added to the strain and tree death, resulting in a drop in forest cover. There is a robust link between decreased precipitation and the drought severity; this underline how the drought has impacted the region's forest cover and led to forest loss [5,13].

Another important factor is elevation; according to the studies, elevations have a serious impact on forest cover growth. Highlands have cool temperatures and more precipitation, making the conditions more promising for forest growth. Several tree species can hold such kinds of climate conditions, and forest cover becomes denser at these elevations; however, the forest cover growth becomes too harsh at the peak altitudes [1,36].

On the other hand, some applications, such as remote detecting and GIS practices, aim to provide a robust output in the case of evaluating or monitoring forest cover shifts. In addition, these practices can be applied to create thematic forest maps, record forest loss ratios, and assess forest deterioration regions. Besides the analysis of satellite imagery alongside other geospatial material, researchers may discover significant instructions about the processes of changing forest cover and develop approaches to promote responsible management of forests [31].

Several studies have been conducted in Erbil province on the changing in forest cover using modern remote detecting technologies, particularly in machine learning models [20,26]. The Random Forests model has developed as an impressive machine learning tool for applying in land use cover classification and change sensing images using satellite imagery such as Landsat 8. Particularly, applying the RF model is less vulnerable to the cloud cover effects compared to other segmentation models when using high-resolution images. Moreover, even at combining both spectral and texture features, RF has confirmed its reliability and accuracy in enhanced image classification [26].

Ahmed (2023) classified forest land into categories in the Amazon rainforest region, attempting a total accuracy of 94.2%, and combined texture structures used from Landsat 7-8 into their RF model, resulting in a noteworthy enhancement in classification accuracy compared to using spectral features alone. Gismatullin et al. (2022) reveled that using the RF model to classify forest land cover in the western Siberian taiga, they reached an accuracy of 92.5% [2,15].

Our main objective of this research is to assess changes in forest cover, including natural and artificial forest in the northeast of Erbil Province between two thematic maps 2003 and 2023 using advanced machine learning techniques.

Methodology

Description of study area

Our research focused on forest cover changes in Erbil province, Kurdistan Region of Iraq (KRI), covering an area of approximately 7,198 Km^2. The study area includes the districts of Shaqlawa, Choman, Soran, and Mergasur in the northeast of Erbil. It is bounded by coordinates ranging from 36° 26′ 7.8″ to 37° 11′ 37″ N and 44° 14′ 44″ to 45° 05′ 25″ E [37] (Figure 1 and Table 1).

The chosen area overall experiences hot, dry summers and chilly, precipitation-filled winters. It is a semi-arid environment. The Koppen climatic classification, however, indicates that mountainous areas at higher elevations have Mediterranean climate characteristics [6].

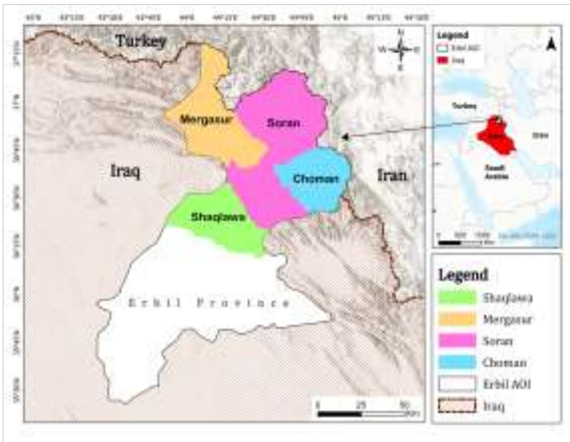

Figure 1. Study area description map adapted by ArcGIS Pro 3 software

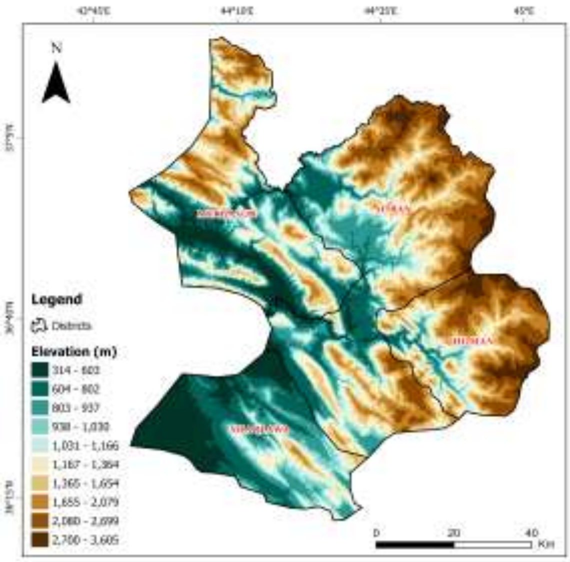

Figure 2. Digital Elevation Model (DEM) of the study area with a 12.5m pixel resolution

Shaqlawa district: is located on the mountainside of Safin Mountain with coordinates 44°13'39"E - 36°23'52"N, in a big valley enclosed with dense forests. Its area is about 1,342 Km^2, it has elevation (313-1945) m at a.s.l. with moderate temperatures, very cold in winter with much rain and snow [18].

Choman district: lies on coordinates 44°50'40"E - 36°37'18"N, has elevation about (594-3605) m a.s.l with area about 1,313 Km^2. The center of the district, is surrounded by a chain of mountains. It has rich forest and beautiful nature.

Soran district: is situated in a rolling plain with coordinates 44°35'15"E - 36°47'36"N, encircled by the Zozik Mountains to the north, Korek Mountains to the south, and Handren Mountains to the east. The district boasts the dense Soran Forest within the Kurdistan Region of Iraq. The climate is characterized by cold winters and hot summers. It has elevation between (372-3487) m at a.s.l. with area about 2,906 Km^2.

Mergasur district: lies in the far North of the Governorate of Erbil at the Iraq-Iran-Turkey triangle with coordinates 44°11'15"E - 36°55'50"N. It is summer are relatively hot, with almost dry weather, and the winter are very cold with heavy rains, with elevation (360-2786) m at a.s.l, and area about 1818 Km^2 [18]. Figure 2 depicts the topography of the study area using DEM image, it covers Shaqlawa, Choman, Soran, and Mergasur districts.

Table 1. Geographic characteristics of study area districts

District	Coordinates (DMS)	Area (Km^2)	*Elevation (m) (Low-High)
Shaqlawa	44°13'39"E 36°23'52"N	1,342	313 – 1,945
Choman	44°50'40"E 36°37'18"N	1,132	594 – 3,605
Soran	44°35'15"E 36°47'36"N	2,906	372 – 3,487
Mergasur	44°11'15"E 36°55'50"N	1,818	360 – 2,786

*Elevation values were extracted from DEM raster with 12.5m resolution using ArcGIS Pro.

Acquiring data

Landsat satellite imagery with 30 m resolution was obtained from the United States of Earth Explorer (USGS) https://earthexplorer.usgs.gov/. The imagery included scenes from Landsat 7 and Landsat 9 for two specific years 2003 and 2023. These imageries were utilized to achieve thematic maps of the study zone (Table 2). This selection allows for a comparative analysis of the study area across a twenty-year timeframe. Our data analysis and preparation were conducted only between two thematic raster images 2003 and 2023 (categorical forest cover change) using a combination of software tools, ArcGIS Pro software, Google Earth Engine (GEE), Excel sheets, and Google Earth Pro.

Table 2. Landsat satellite imagery details (2003 & 2023)

Satellite	No. of scene	RGB	False color (CIR)	Path	Row	Data acquired	Resolution (Each pixel)
Landsat 7 (2003)	8	Red Green Blue	B4 (NIR) B3 (Red) B2 (Green)	169	34+35	Landsat 7 ETM+ C2 L1 August 2003	30m X 30m
Landsat 9 (2023)	8	Red Green Blue	B5 (NIR) B4 (Red) B3 (Green)	169	34+35	Landsat 9 OLI/TIRS C2 L1 August 2023	30m X 30m

NDVI, SAVI, and BSI Indices

The indices, such as NDVI (Normalized Difference Vegetation Index), SAVI (Soil Adjusted Vegetation Index), and BSI (Bare Soil Index), were obtained from the Google Earth Engine Platform (GEE) for both years (2003 and 2023). The raster data for these indices have a 30-meter pixel resolution, and atmospheric correction was applied to all the rasters [19,39,40]. The purpose of these indices is to identify and analyze forested and non-forested land areas (Table 3 and Figure 10).

Table 3. Comparison of NDVI, SAVI, and BSI; Spectral Bands, Equations, and Applications

Index	Used band	Equation	Used case & purpose
NDVI	NIR, Red	$NDVI = \frac{(NIR - Red)}{(NIR + Red)}$	Dense vegetation and agriculture Measures vegetation health
SAVI	NIR, Red, Soil factor (L)	$SAVI = \frac{(NIR - Red)}{(NIR + Red + L)} \times (1 + L)$	Soil erosion and urban expansion Reduces soil background effects
BSI	Red, NIR, SWIR, Blue	$BSI = \frac{(Red + SWIR) - (NIR + Blue)}{(Red + SWIR) + (NIR + Blue)}$	Sparse vegetation and arid regions Highlights bare soil

Resources: Tucker (1979), Huete (1988), and Zha *et al.* (2003)

Random Forest Algorithm & False Color Infrared Image (CIR)

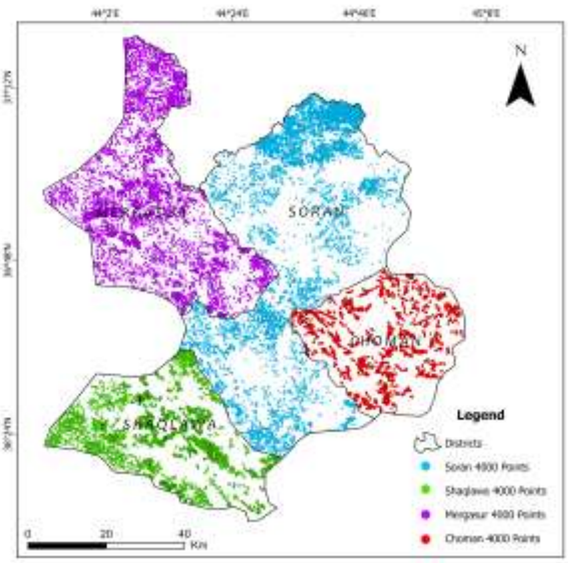

Our work focused on categorical forest cover change between two thematic maps in the four Erbil's districts for 2003 and 2023. A supervised classification Random Forest algorithm (RF) used for forest cover change analyses through recall of Landsat satellite imagery. The land cover adapted and classified into two main classes: forest land and non-forest land for each district. For each district, we created 4,000 sample training points for each class (forest and non-forest), resulting in a total of 8,000 points per district. Across the four districts, this amounted to 32,000 sample training points, which were used to train the RF model and generate accurate land cover classification maps. These training points were applied to False Color Infrared (CIR) images for both 2003 and 2023 using ArcGIS Pro software, enabling us to visualize and analyze changes in forest cover over the two-decade period across the four northeastern districts of Erbil (Figure 3).

Figure 3. Sample training points for four districts

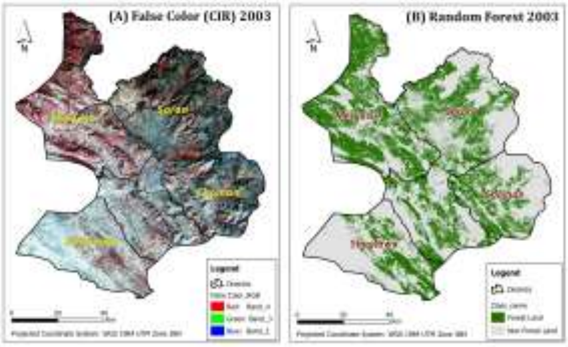

RF was employed to analyze the spectral information within the acquired Landsat imagery, particularly focusing on False Color Infrared (CIR) bands; (band5; near-infrared, band4; red, and band3; green), Figure 4&5B. On the other hand, false color combination image, are a picturing technique that improves the illustration of vegetation healthiness, dark red areas on the false image represents healthy vegetation areas as shown in figure 4&5A [9].

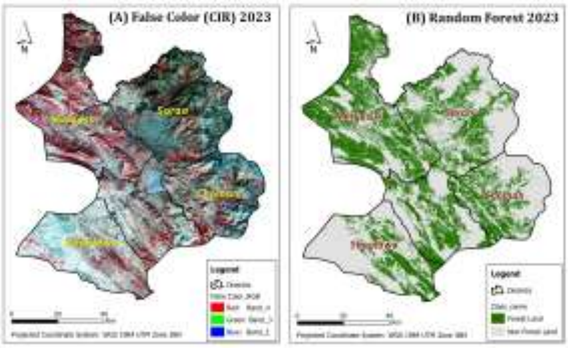

Figure 4. (A) False color image and (B) RF (2003)

Figure 5. (A) False color image and (B) RF (2023)

Three bands were used for false color image; near-infrared, visible red, and short-wave infrared, to the red, green, and blue channels respectively. It allows for us a purer division between healthy and stressed vegetation due to the exceptional spectral reflectance patterns [22,28]. The shapefile boundaries of districts were created manually from ArcGIS Pro based on software basemaps for each of Shaqlawa, Choman, Soran, and Mergasur. Then, their areas were then calculated and added to their attribute tables, then WGS UTM 38N projected coordinate system were applied for all the shapefiles.

The lands of non-forest combined in one class such as built-up areas, water bodies, barren soils, rocks, growing crops, and grasslands. While the forest land class is representing forest land (dense forest and open/shrubland forest). Later, the techniques of categorical change detection wizard were generated between two thematic maps 2003 and 2023 to measure and map the lands that changed, including four classes; forest land (unchanged), forest land to non-forest land, non-forest land (unchanged), and non-forest land to forest land [37]. Figure 6, flowchart describes the detail steps and processes of methodology for the study area by using the powerful machine learning (Random Forest).

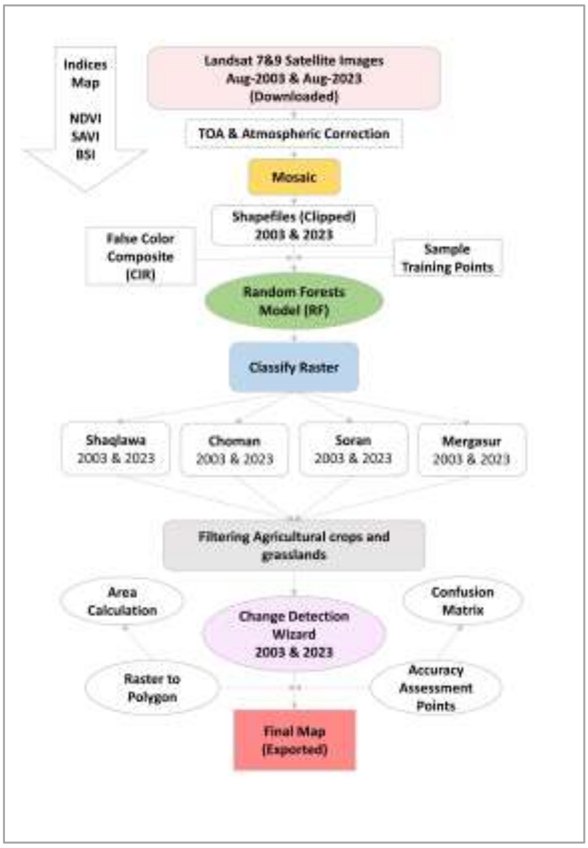

Figure 6. Flowchart of the methodology

Accuracy assessment & confusion matrix

Random sampling points are generated for accuracy assessment calculation for all districts in the region. The amount of assessment points was 500 for each class. Our map class was divided into two main classes: forest land and non-forest land. After that, the assessment points were compared with high-imagery software called Google Earth Pro. The software has historic reference imagery maps that lead to movement and transition between preview years. The points that were taken for the assessment refer to the real locations on the reference imagery map, providing reference data for the land cover class of each sample point, such as tree cover and land use features [27]. The confusion matrix was used after creating reference points. The purpose of using the confusion matrix is to provide an initial component for accuracy assessment processing that presents detailed data of how the model classified and worked for both land cover classes. These data express the classification of correct pixel quantity and the quantity of unclassified pixels in the map as well [8,29]. The output of the confusion matrix table includes metrics of overall accuracy; the table indicates the correct number of classified pixels in the map. Another part of the table is producer's accuracy and user's accuracy. Both used as percentages in the table, producer's accuracy shows the probability that a pixel considered as an exact class in the reference data is properly classified in the result. Moreover, the producer's accuracy deals with the model's facility to correctly identify pixels. It also shows how well the model classifies the correct pixels within a certain class, while the user's accuracy assesses the reliability of the model's assigned class labels. It also evaluates the uniformity of the model's classification. This represents how the majority of pixels belonged to the correct class; it expresses the likelihood that a pixel classified as an exact class in the result section actually implies that class in the reference imagery map [34,38].

Research limitation

Landsat 9 satellite images offer improved geometric accuracy, enhanced radiometric calibration, fewer artifacts, and better temporal and spatial resolution compared to older satellite imagery, such as MODIS, Landsat 7, and Landsat 8, due to advancements in satellite imagery processing. However, in highly complex areas with varied vegetation types, the 30m × 30m pixel resolution (900 m^2) may not capture all the detailed variations on the ground due to pixel limitations. These limitations can potentially lead to underestimation or overestimation in the output data for forest land change, particularly in areas with gradual or subtle changes in forest composition [12].

Result & Discussion

Forest cover change classification

Table 4 presents the forest cover changes in four districts of Erbil Governorate from 2003 to 2023. The data reveals considerable forest loss across all districts. Soran District experienced the highest total forest cover loss with 246 Km^2 converted to non-forest land (8.45%), followed by Mergasur (130 Km^2, 7.14%), Choman (72 Km^2, 6.35%), and Shaqlawa (59 Km^2, 4.38%). While all districts also experienced forest regeneration (Non-Forest Land to Forest Land), the gains were significantly lower than the losses, indicating a net decline in forest cover.

Table 4. Area (Km^2) of forest cover classes in Shaqlawa, Choman, Soran, and Mergasur districts (2003 & 2023)

Class	Shaqlawa District		Choman District		Soran District		Mergasur District		SUM	
	Area (Km^2)	%	Area (Km^2)	%	Area (Km^2)	%	Area (Km^2)	%	Area (Km^2)	%
Forest Land (Non-changed)	307	22.85	333	29.41	843	28.99	918	50.49	2,400	33.34
Forest Land to Non-Forest Land	59	4.38	72	6.35	246	8.45	130	7.14	506	7.03
Non-Forest Land to Forest Land	50	3.72	75	6.64	217	7.48	146	8.05	489	6.79
Non-Forest Land (Non-changed)	927	69.06	652	57.60	1,601	55.07	624	34.33	3,803	52.84

SUM	**1,342**	**100**	**1,132**	**100**	**2,906**	**100**	**1,818**	**100**	**7,198**	**100**

Figure 7 shows the Landsat satellite imagery was used to analyze the forest cover change in the four districts of Erbil province: Shaqlawa, Soran, Choman, and Mergasur between 2003 and 2023.

In this study thematic maps created through a machine learning algorithm named (Random Forests), the classification for each map divided into four categories, are (forest land (unchanged); forest land to non-forest land, non-forest land to forest land, and non-forest land (unchanged). Several academics applied Random Forests Model in their researches, according to the Joshi et al. (2023) they classified their study area into different categories using Landsat data and Random Forest Model, the model has clear benefits for handling multispectral data and creating accurate thematic maps [23]. Also, Mykola et al. (2016) work on land cover interpretation using Landsat imagery [32].

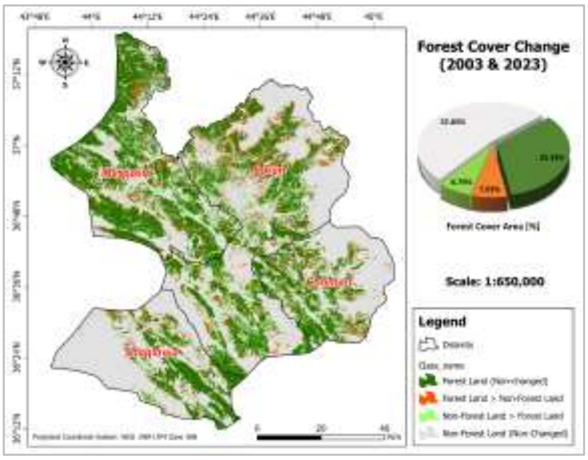

Figure 7. Forest cover change map (2003 & 2023), the study area in northeastern Erbil

Forest change distribution in all districts is shown in the (Figure 8) A, B, C, and D. A considerable portion of the land has experienced forest loss, however the bulk of the land in all districts is still non-forest land (unchanged), ranging from 34.33% to 69.06%). The Soran region has the highest rate of forest loss, accounting for 8.45% of the total. Mergasur (7.14%), Choman (6.35%), and Shaqlawa (4.38%) are the next highest rates. The amount of forest regeneration (from non-forest land to forest land) is somewhat evident, although it is still far less than the total amount of forest loss throughout all districts. Whereas chart E examines these variations for the four districts as a whole, chart F represents the entire forest cover distribution, illustrating the dominance of non-forest land (59.87%) and the increasing impact of forest loss (7.03%) across the area. As highlighted by the land cover alteration is a complex phenomenon with vital environmental and ecological consequences. The loss of Forest cover shares in climate change by reducing carbon storing capacity. Moreover, it leads to a series of negative impacts, for example, soil erosion, water scarcity, and reduced agricultural outcomes [7].

Rash et al., (2023) were used machine learning algorithms (MLAs) for land use/land cover classification for north-east of Erbil, the Random Forest (RF) algorithm obtaining the highest overall accuracy (OA) of 97. 47% and a kappa coefficient (Kc) reaching from 0. 93 to 0. 97 across the study sessions. However, other algorithms like Artificial Neural Network (ANN), Support Vector Machine (SVM), Extreme Gradient Boosting (XGBoost), and K-Nearest Neighbor (KNN), achieved well but with slightly lower accuracy than RF algorithm. On the other hand, increasing the amount of forest cover provides a strong solution. Additionally, carbon sinks into forests assist in slow down worldwide warming, improve soil quality, and increase agricultural productivity [10].

Besides, understanding the complex causes of deforestation or forest loss is crucial because it allows us to recognize the fundamental causes and take suitable action against them, including agricultural development, climate change, forest fires, urbanization and even reduced precipitation caused by deforestation itself. Based on the observed trends, the region's forest cover may continue to drop in the western regions as a result of agricultural growth, while it may remain steady or even grow in the eastern districts. Future studies should examine focused interventions and flexible land-use regulations that strike a balance between agricultural requirements and forest preservation in order to promote sustainable forest management [26,33].

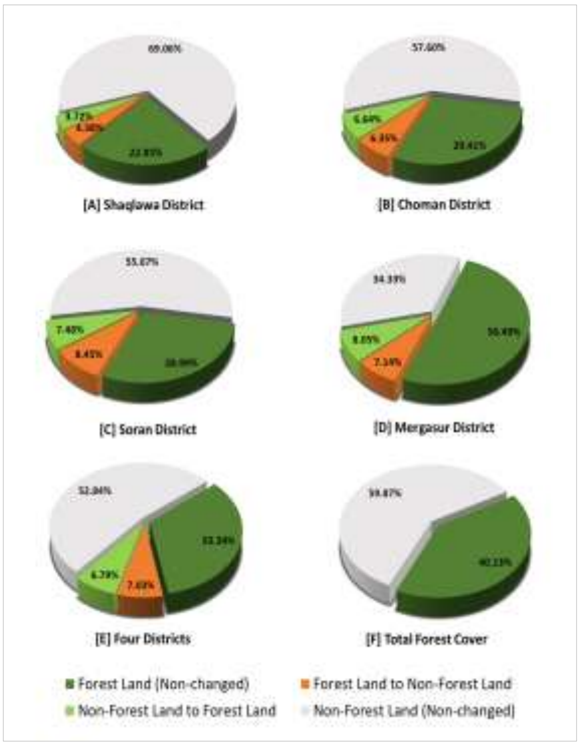

Figure 8. Percentages and total of forest cover change areas in four districts (2003 & 2023)

NDVI, SAVI, and BSI

Figure 9 compares the vegetation and soil index maps for August 2003 and August 2023, derived from Landsat 7 and Landsat 9 data for the same geographic area. The results reveal significant changes in land cover and vegetation density over the 20-year period, emphasizing the impact of environmental and anthropogenic factors on the study area [19,39,40]. These noticeable changes indicate that the region has experienced environmental stress and land-use transformations over the two decades. The NDVI and SAVI maps vividly illustrate the locations of vegetation changes, while the BSI specifically highlights areas of soil degradation and erosion over time. This information is critical for interpreting the changes detected by the Random Forest (RF) classification map, as well as the false color composite images of the study area. The dark green areas on the maps represent healthy vegetation with consistently high index values and dense coverage.

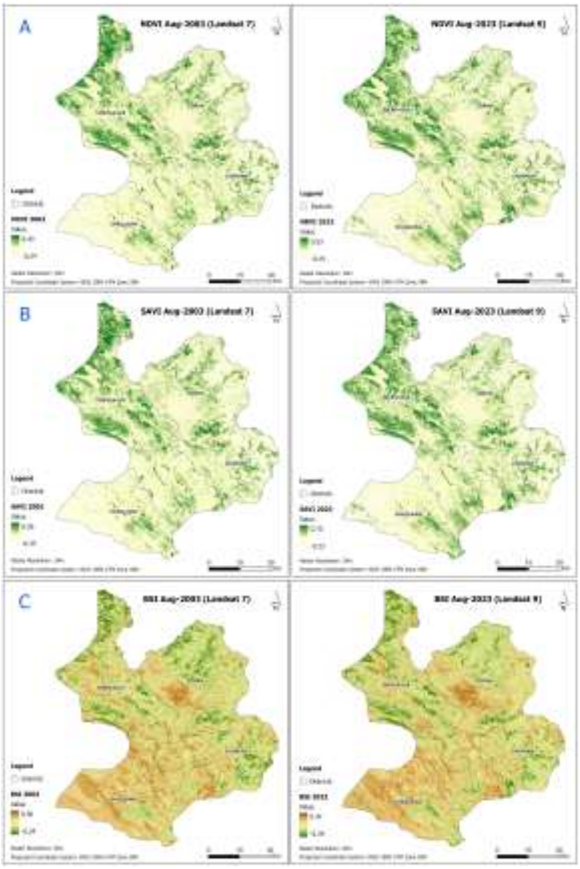

Figure 9. Spatio-temporal comparison 2003 and 2023 of (A) NDVI, (B) SAVI, and (C) BSI maps

Accuracy assessment of land cover classification

Accurately assessing forest cover change is essential for informed decision-making, targeted conservation efforts, and understanding the drivers of deforestation. This study employed high image quality from Google Earth software as ground truth data reference, acknowledging the limitations inherent to this approach [30]. To ensure classification accuracy, assessment points were created, followed by the implementation and validation of a confusion matrix using reference data derived from Google Earth Pro imagery. Table 5 showed that the overall classification accuracy in 2003 was 88%, whereas overall classification accuracy in 2023 was 93%. Khan et al., (2022), they informed a high kappa coefficient (Kc) ranging from 0.93 to 0.97. Ge et al., (2020), both RF and ANN accomplished a high Kc of 0.96, indicating effective classification [14,25].

Table 5. Accuracy assessment and confusion matrix of forest cover classification

District	Year	Class	FL	NFL	Total	UA	Ka
Shaqlawa District	2003	FL	37	1	38	0.97	
		NFL	13	49	62	0.79	
		Total	50	50	100		
		PA	0.74	0.98		0.86	
		Ka					0.72
	2023	FL	40	5	45	0.89	
		NFL	3	52	55	0.95	
		Total	43	57	100		
		PA	0.93	0.91		0.92	
		Ka					0.84
Choman District	2003	FL	22	1	23	0.96	
		NFL	11	66	77	0.86	
		Total	33	67	100		
		PA	0.67	0.99		0.88	
		Ka					0.71
	2023	FL	27	4	31	0.87	
		NFL	3	66	69	0.96	
		Total	30	70	100		
		PA	0.90	0.94		0.93	
		Ka					0.83
Soran District	2003	FL	18	2	20	0.90	
		NFL	8	72	80	0.90	
		Total	26	74	100		
		PA	0.69	0.97		0.9	
		Ka					0.72
	2023	FL	24	3	27	0.89	
		NFL	3	70	73	0.96	
		Total	27	73	100		
		PA	0.89	0.96		0.94	
		Ka					0.85
Mergasur District	2003	FL	22	7	29	0.76	
		NFL	5	66	71	0.93	
		Total	27	73	100		
		PA	0.81	0.90		0.88	
		Ka					0.70
	2023	FL	24	1	25	0.96	
		NFL	5	70	75	0.93	
		Total	29	71	100		
		PA	0.83	0.99		0.94	
		Ka					0.85

FL=Forest Land, NFL=Non-Forest Land, UA=User Accuracy, PA=Producer Accuracy, Ka=Kappa coefficient

Conclusion

Our research demonstrates that the Random Forest (RF) algorithm is among the most accurate models for identifying forested areas. Additionally, vegetation and soil indices, including NDVI, SAVI, and BSI, proved valuable for visualizing and assessing vegetation health and bare soil areas. The findings revealed significant spatial heterogeneity in forest dynamics, emphasizing the importance of spatially explicit analyses for understanding forest cover variability within a region. The study identified two major types of changes: forest loss and forest gain. Forest loss, particularly in the western region of Erbil, is a critical concern due to its direct impacts on climate change, soil health, and regional ecosystems. Key drivers of this loss include agricultural expansion, urbanization, rainfall deficiency, drought, overgrazing, and forest fires. These findings highlight the urgent need for comprehensive strategies to address forest degradation. Further research is necessary to better understand the underlying causes of forest cover changes in the region. Integrating climate and land use projections into forest cover transition models could provide valuable insights for sustainable forest management and long-term planning.

References

[1] Ahmed, A., Hamzah, Y., & Mohammed, T. (2013). The relationship between forest cover and elevation in the Kurdistan Region of Iraq. International Journal of Environmental Science and Technology.

[2] Ahmed, M. A. (2023). Assessment of forest cover changes in Kurdistan Region of Iraq using Landsat satellite imagery. Environmental Monitoring and Assessment.

[3] Ahmed, M., Yousif, A. A., Al-Mahmood, M. J., Omer, F. K., & Hussein, A. K. (2019). Rainfall trends and variability in the Kurdistan Region of Iraq. Climate Change.

[4] Ahmed, S., Jafar, Z., Omer, K., & Mustafa, D. (2018). Forest cover change in the Kurdistan Region of Iraq (KRI): A remote sensing analysis. Journal of Applied Remote Sensing.

[5] Allen, C. D., Breshears, D. D., & McDowell, N. G. (2010). Global changes in drylands: A review of rates and drivers. Ecosphere.

[6] Beck, H. E., Zimmermann, N. E., McVicar, T. R., Vergopolan, N., Berg, A., & Wood, E. F. (2018). Present and future Köppen-Geiger climate classification maps at 1-km resolution. Scientific Data. https://doi.org/10.1038/sdata.2018.214

[7] Canadell, J. G., & Raupach, M. R. (2008b). Managing forests for climate change mitigation. Forest Ecology and Management.

[8] Congalton, R. G., & Green, K. (2009). Assessing the accuracy of remotely sensed data: Principles and practices (2nd ed.). CRC Press. https://doi.org/10.1201/9781420055139

[9] Escada Filho, F. M., de Freitas, J. A., & Coelho, M. M. (2008). Assessing the use of false-color infrared composites for sugarcane stress detection. International Journal of Remote Sensing.

[10] Evans, J. (2009). The role of forests in watershed protection. In Forests and Society: Recognizing the Benefits from Forests. Springer.

[11] FAO. (2020). Global Forest Resources Assessment 2020. Food and Agriculture Organization of the United Nations.

[12] Fu, B., Wang, Y., Wang, Y., Li, Z., & He, H. (2022). Capability assessment of Landsat-9 Operational Land Imager (OLI-2) for land cover classification. Remote Sensing.

[13] Gaznayee, A. H. (2022). A Geospatial Approach for Analysis of Drought Impacts on Vegetation Cover and Land Surface Temperature in the Kurdistan Region of Iraq. Journal of Water and Environmental Management. https://doi.org/10.3390/w14060927

[14] Ge, G., Shi, Z., Zhu, Y., Yang, X., & Hao, Y. (2020). Land use/cover classification in an arid desert-oasis mosaic landscape of China using remote sensed imagery: Performance assessment of four machine learning algorithms. Global Ecology and Conservation. https://doi.org/10.1016/j.gecco.2020.e00971

[15] Gismatullin, R., Zhuravin, V., & Korovkin, A. (2022). Random Forest and Support Vector Machine Algorithms for Land Cover Classification of the Western Siberian Taiga Using Landsat 8 Data. Forests.

[16] Hamad, S. R., Al-Ansari, N., Knutsson, S., & Laue, J. (2022). Trend analysis of rainfall and temperature in the Kurdistan Region of Iraq. Journal of Water and Climate Change.

[17] HamadAmin, B. A., & Khwarahm, N. R. (2023). Mapping Impacts of Climate Change on the Distributions of Two Endemic Tree Species under Socioeconomic Pathway Scenarios (SSP). Sustainability. https://doi.org/10.3390/su15065469

[18] Hawler Governorate. (2024). [Hawler Governorate]. https://www.hawlergov.org/app/.

[19] Huete, A. R. (1988). A soil-adjusted vegetation index (SAVI). Remote Sensing of Environment. https://doi.org/10.1016/0034-4257(88)90106-X

[20] Ibrahim, A. E., & Azeez, D. R. (2024). Land Cover and Land Use Changes Study of Shwan and Altun Kopre areas in Kirkuk governorate. Kirkuk University Journal for Agricultural Sciences (KUJAS).

[21] Jafar, Z., Omer, K., & Mustafa, D. (2019). Assessment of forest cover change and its impact on ecosystem services in the Kurdistan Region of Iraq. In Geospatial Technology for Sustainable Development. Springer, Singapore.

[22] Jensen, J. R. (2016). Introductory digital image processing: A remote sensing perspective. Pearson Education Limited.

[23] Joshi, A., Smith, B., & Johnson, C. (2023). Classification of study areas using Landsat data and Random Forest Model (RF) for accurate thematic mapping. Journal of Remote Sensing and Geospatial Analysis, 15(3), 245-260.

[24] Keenan, R. J., Reay, D. S., Achard, F., Meir, P., & Kirubi, C. (2015). Woody biomass and carbon densities of forests worldwide. Proceedings of the National Academy of Sciences.

[25] Khan, A., & Sudheer, M. (2022). Machine learning-based monitoring and modeling for spatio-temporal urban growth of Islamabad. The Egyptian Journal of Remote Sensing and Space Science. https://doi.org/10.1016/j.ejrs.2022.03.012

[26] Khwarahm, N. R., Qader, S., Ararat, K., & Fadhil Al-Quraishi, A. M. (2021). Predicting and mapping land cover/land use changes in Erbil /Iraq using CA-Markov synergy model. Earth Science Informatics. https://doi.org/10.1007/s12145-020-00541-x

[27] Lausch, A., Heurich, M., Gordalla, D., Dobner, H. J., Gwillym-Margianto, S., & Pause, M. (2016). Linking satellite-based and in-situ observations for understanding forest landscape change. Remote Sensing of Environment.

[28] Lillesand, T. M., & Kiefer, R. W. (2000). Remote sensing and image interpretation. John Wiley & Sons.

[29] Liu, C., Frazier, P., & Kumar, S. (2007). Comparative evaluation of semantic segmentation algorithms for object-based land cover classification. International Journal of Remote Sensing.

[30] Luque, A. M., Carrillo, D., & Silva, M. J. (2008). Land cover and change analysis using Google Earth imagery in a Mediterranean landscape. Remote Sensing of Environment.

[31] Massetti, M., Ferretti, M., & Chiesi, M. (2020). Monitoring forest cover change and its drivers in Mediterranean ecosystems using Landsat time series. Remote Sensing.

[32] Mykola, A., Palii, I., & Tereshchenko, A. (2016). Using the Random Forest Classification for Land Cover Interpretation of Landsat Images in the Prykarpattya Region of Ukraine. Procedia Environmental Sciences.

[33] Ozturk, M., Sahin, E., & Aydin, H. (2020). Forest cover change analysis of the Kurdistan Region of Iraq using Landsat imagery (1984-2020). Environmental Monitoring and Assessment.

[34] Pontius Jr, R. G., & Millington, K. A. (2011). Comparison of accuracy assessment techniques for object-based classification. Remote Sensing of Environment.

[35] Radha, K. O., & Khwarahm, N. R. (2022). An Integrated Approach to Map the Impact of Climate Change on the Distributions of Crataegus azarolus and Crataegus monogyna in Kurdistan Region, Iraq. Sustainability. https://doi.org/10.3390/su142114621

[36] Rahmani, H., Chen, X., & Rogan, J. (2014). Satellite remote sensing for monitoring deforestation and forest degradation in the Zagros Mountains of Kurdistan, Iraq. International Journal of Remote Sensing.

[37] Rash, A., Mustafa, Y., & Hamad, R. (2023). Quantitative assessment of Land use/land cover changes in a developing region using machine

learning algorithms: A case study in the Kurdistan Region, Iraq. Heliyon. https://doi.org/10.1016/j.heliyon.2023.e21253
[38] Reddy, C. S., Sreekanth, P. S., Jha, C. S., & Dadhwal, V. K. (2010). An overview of accuracy assessment techniques for classification in remote sensing. International Journal of Applied Earth Observation and Geoinformation.
[39] Tucker, C. J. (1979). Red and photographic infrared linear combinations for monitoring vegetation. Remote Sensing of Environment. https://doi.org/10.1016/0034-4257(79)90013-0
[40] Zha, Y., Gao, J., & Ni, S. (2003). Use of normalized difference built-up index in automatically mapping urban areas from TM imagery. International Journal of Remote Sensing. https://doi.org/10.1080/01431160304987